Engineering Geology 152 (2013) 10–16

Contents lists available at SciVerse ScienceDirect

Engineering Geology

journal homepage: www.elsevier.com/locate/enggeo

Engineering properties of a vertisolic expansive soil deposit

Maki Ito, Shahid Azam *

Environmental Systems Engineering, Faculty of Engineering and Applied Science, University of Regina, 3737 Wascana Parkway Regina, SK, Canada S4S 0A2

ARTICLE INFO

Article history:
Received 13 June 2012
Received in revised form 23 September 2012
Accepted 13 October 2012
Available online 22 October 2012

Keywords:
Vertisolic soil
Water retention
Volume change
Soil microstructure

ABSTRACT

Vertisolic expansive soils are characterized by unique morphological features and extensive volume changes of swelling clay minerals. The engineering properties of such a soil deposit in Regina, Canada, were investigated under in situ conditions. Results indicated a bi-modal SWCC composing of a fissure AEV (10 kPa) and a matrix AEV (300 kPa based on water content and 6000 kPa based on degree of saturation). The latter value matched the field water content and the plastic limit, of which both occurred at $S_{ave} \approx 80\%$. The swell-shrink path was found to be S-shaped and included a low structural shrinkage ($S_{ave} = 100\%$ to $S_{ave} = 80\%$ at w_p) followed by a sharp decline during normal shrinkage ($S_{ave} = 80\%$ to $S_{ave} = 60\%$ at w_s) and then by a low decrease during residual shrinkage ($S_{ave} = 60\%$ to $S_{ave} = 0\%$). An equilibrium soil microstructure for the undisturbed samples mean that for the field conditions (up to the matrix AEV), the soil aggregates remain fully saturated whereas drainage and volume changes primarily occur through the fissures.

1. Introduction

Vertisolic expansive soils are characterized by unique morphological features and extensive volume changes of swelling clay minerals (Brierley et al., 2011). A typical example of such deposits is the Regina clay (Saskatchewan, Canada) that evolved due to geologic weathering of glacio-lacustrine sediments under restrained leaching in a semi-arid climate (Christiansen and Saure, 2002). The soil is primarily composed of expansive clay minerals (such as smectite, illite, and chlorite) and exhibits high water adsorbing and water retention capabilities. The surface layer of the clay has extensive fissuring that is derived from moderate over-consolidation as well as alternate swell-shrink and freeze–thaw cycles (Ito and Azam, 2010). Stress induced particle rearrangement has resulted in localized wedge-shaped aggregates bounded by slickensides. The hairline discontinuities especially influence heaving and subsidence in the top stratum of the deposit where most of the construction occurs. Being in contact with the atmosphere, volume changes in this layer are governed by seasonal weather variations, that is, by periodic saturation and desaturation.

Alternate swelling and shrinkage in Regina clay has impaired civil infrastructure such as transportation networks (Kelly et al., 1995), residential, industrial, and commercial facilities (Azam and Ito, 2007), and water supply and sewage collection systems (Hu and Hubble, 2005). Damages to engineered facilities are clearly manifested in the form of differential heave in roadways and sidewalks, inclined cracking in slab-on-grade basements and masonry walls, and fatigue and breakage in underground storage tanks and buried pipelines. The associated repair cost is usually quite enormous. For example, the breakage rate in the 850 km long water supply network in the city has now reached a 30-year maximum of 0.27 breaks/km/year, costing more than $2 million in annual maintenance. To ensure an uninterrupted infrastructure utility, there is a need to understand the volume change behavior of the indigenous deposit.

The main objective of this paper was to investigate the engineering properties of Regina clay under in situ conditions. First, the geotechnical index properties were determined for preliminary soil assessment. Second, the soil water characteristics curve (SWCC) was determined to understand the water retention capacity of the soil. Third, the swell-shrink test was conducted to study soil volume changes during saturation–desaturation. Finally, scanning electron microscopy was conducted for selected samples to correlate soil microstructure with engineering behavior.

2. Geologic evolution of the deposit

The Quaternary period in southern Saskatchewan was governed by a series of glacial events that, in turn, were responsible for erosion of the Cretaceous and Tertiary rocks and their subsequent deposition to form the indigenous glacial drift. The drift consists of the following three groups from older to younger (Christiansen and Saure, 2002): Empress (gravel and sand), Sutherland (till and stratified deposits), and Saskatoon (till, gravel, sand, silt, and clay). Alternate scraping, deposition, overburdening, and reworking of materials by up to seven glacial advances and retreats resulted in extensive particle disintegration. The present-day surface soils in the Regina area formed during the last glaciation known as the Wisconsinan (23,000 years B.P. to 17,000 years B.P) that covered the entire province. The ice sheet started to retreat in the northeastwardly direction around 17,000 years B.P. The rate of ice meltdown was initially about 60 m/year and gradually increased to 275 m/year in the final stages. According to Mollard et al.

* Corresponding author. Tel.: +1 306 337 2369; fax: +1 306 585 4855.
E-mail address: Shahid.Azam@URegina.CA (S. Azam).

0013-7952/$ – see front matter © 2012 Elsevier B.V. All rights reserved.
http://dx.doi.org/10.1016/j.enggeo.2012.10.004

(1998), this process was completed around 8000 years B.P. when the essential features of the present landform emerged including moraines (a raised ground covering of unsorted till) and eskers (a long winding ridge of sorted sands and gravel). These ground features bounded the proglacial Regina Lake where fine-grained soils gradually settled at the basin floor during the Wisconsinan to develop a homogeneous clay deposit of up to 12 m depth. Subsequent wet–dry and freeze–thaw cycles, alluvial and fluvial transportation processes and the presence of salt-forming ions further modified the deposit during the postglacial period. Overall, the soil preserved the pre-existing expansive clay minerals such as smectite, illite and chlorite due to restrained leaching in the Lake and the prevalent aridity in the area (Ito and Azam, 2009).

The indigenous clay deposit has a spatially variable stress distribution because of the following reasons: (i) geologic rebound of the deposit due to removal of up to 1000 m thick glacial cover; (ii) swelling and shrinkage of clay minerals due to water hydration and dehydration in spring and summer; and (iii) heave and subsidence of the soil layers due to ice lens formation and decay in winter and spring. Ito and Azam (2009) reported that the average vertical swelling pressure in the surface layer (1.2 m deep and a vertical overburden pressure of 20 kPa) of the clay is 120 kPa. Since this soil layer is laterally confined, the lateral earth pressure is expected to be higher than the vertical overburden pressure (Hong, 2008). Whereas no data is available for the local soil deposit, in situ measurements by Brackley and Sanders (1992) indicated that the lateral pressure in surficial expansive clays (2 m deep) is up to four times the vertical pressure. Such passive conditions imply localized shearing failure during alternate volume changes due to seasonal weather variations. The internal movement occurs in multiple directions (20° to 60° with the horizontal) thereby developing a network of intersecting shear planes. These slickensides form the boundaries of wedge-shaped aggregates with a central low and a circumferential high because of material oozing outwards and upwards along the weak boundaries (Brierly et al., 2011). Successive swell-shrink cycles render these soil features quite permanent and conspicuous particularly in the surface layer. This is the case with the local clay deposit that exhibits extensive soil fissuring (up to 2 mm wide) with inconsistent lateral spacing and variable dip angles in the top 1.5 m depth.

The stress related morphology in vertisolic expansive soils is initiated at the microstructural level and is governed by the clay mineral type and the amount of clays and non-clays such as silts, salts, carbonates, and organics (Ahmad and Mermut, 1996). The overall soil matrix is characterized by a random arrangement of plasma (clay particles generally finer than 0.002 mm) usually forming a sepic fabric (anisotropic domains of clay particle booklets) with several striated interference patterns (Douglas, 1990). The primary conspicuous morphological features in such soils include the following (Fitzpatrick, 1993): (i) vosepic zones of plasma separation along the larger voids with striations largely parallel to the walls of the voids; (ii) skelsepic zones of plasma accumulation near the surface of coarse skeletal grains eventually forming galaxies or comet tails; and (iii) masepic zones of elongated striations within the plasma as a precursor to a vosepic zone. In addition to these stress induced features, the plasma fabric undergoes periodic changes due to wet–dry cycles. According to Cui et al. (2006), the sepic fabric during swelling is characterized by a face-to-edge particle arrangement due to water hydration of the negatively charged surfaces of expansive clay minerals. This microstructure collapses during shrinkage due to water removal between adjacent clay surfaces and results in a predominantly face-to-face particle arrangement.

3. Research methodology

Undisturbed samples were obtained using the ASTM Standard Practice for Thin-Walled Tube Sampling of Soils for Geotechnical Purposes (D1587-08) from a depth of 0.6 m to 1.2 m. Individual specimens were plastic-wrapped and wax-coated and the entire collection was transferred and stored at the University of Regina as per the ASTM Standard Practice for Preserving and Transporting Rock Core Samples (D5079-08).

3.1. Geotechnical index properties

The geotechnical index properties were determined for preliminary soil assessment and for use in subsequent laboratory investigations according to the ASTM test methods as follows: (i) field water content (w) by the Standard Test Methods for Laboratory Determination of Water (Moisture) Content of Soil and Rock by Mass (D2216-05); (ii) field dry unit weight (γ_d) by the Standard Test Method for Density of Soil in Place by the Drive-Cylinder Method (D2937-10); (iii) specific gravity (G_s) by the Standard Test Methods for Specific Gravity of Soil Solids by Water Pycnometer (D854-10); (iv) liquid limit (w_l), plastic limit (w_p) and plasticity index (I_p) by the Standard Test Methods for Liquid Limit, Plastic Limit, and Plasticity Index of Soils (D4318-10); (v) shrinkage limit (w_s) by the Standard Test Method for Shrinkage Factors of Soils by the Wax Method (D4943-08); and (vi) grain size distribution by the Standard Test Method for Particle-Size Analysis of Soils (D422-63(2007)).

3.2. Soil water characteristic curve

The SWCC was determined according to the ASTM Standard Test Methods for Determination of the Soil Water Characteristic Curve for Desorption Using a Hanging Column, Pressure Extractor, Chilled Mirror Hygrometer, and/or Centrifuge (D6836-02(2008)e2) using about 10 mm thick specimens obtained from the undisturbed core samples. Predetermined suction values were applied using pressure plate/membrane extractors manufactured by Soil Moisture Equipment Inc. These included the following: (i) a 5 bar pressure plate extractor (Model 1600) along with a 0.5 bar porous plate (0675 Series) for 30 kPa suction and a 3 bar porous plate (0675 Series) for 100 kPa and 200 kPa suction; (ii) a 15 bar pressure plate extractor (Model 1500F1) and a 5 bar porous plate (0675 Series) for 300 kPa, 400 kPa, and 500 kPa suction; and (iii) a 100 bar pressure membrane extractor (Model 1020) and a cellulose membrane (1041D21) for 2000 kPa and 6000 kPa suction. The porous plates and the cellulose membranes were submerged in distilled and de-aired water for 24 h to expel air bubbles. Thereafter, the specimens along with the retaining ring were placed on their respective porous plate or cellulose membrane and allowed to saturate in water. Next, the excess water was removed and each porous plate or membrane was placed in the designated extractor. For each suction value, the expelled water from the samples was monitored in a graduated burette. When two consecutive readings nearly matched over a 24 hour period, the test was terminated and the sample water content was determined.

The dew point potentiameter (WP4-T) was used for suction measurement at low water content. The sampling cup was half filled with soil to ensure accurate suction measurement (Leong et al., 2003) by using about 5 mg of material with a known water amount. The unsaturated sample was forwarded to the head space of the sealed measurement chamber, set at 25 °C temperature, through a sample drawer and was allowed to equilibrate with the surrounding air. Equilibration was usually achieved in 10 min to 20 min, as detected by condensation on a mirror and measured by a photoelectric cell. From knowledge of the universal gas constant, R (8.3145 J/mol°K), sample temperature, T (°K), water molecular mass, X (18.01 kg/kmol), and the chamber relative humidity, p/p_o, soil suction was calculated ($\psi = RT/X\ ln(p/p_o)$) and displayed on the potentiameter screen. The water content of the soil was measured as described earlier.

3.3. Swell-shrink test

The swell-shrink test was conducted in accordance with the ASTM Standard Test Method for Shrinkage Factors of Soils by the Wax Method (D4943-08). To obtain the void ratio, the volume of soil specimens was determined using the water displacement method. Each specimen was coated with molten microcrystalline wax ($G_s = 0.9$) and allowed to cool down at room temperature. After wax solidification, the sample was submerged in a 250 ml graduated cylinder that was filled with distilled water. The water height in the cylinder was carefully recorded using a Vernier caliper before and after sample submersion in the cylinder. A graduated syringe was used to remove the increased amount of water displaced by the sample thereby bringing the water height back to the initial reading. The displaced water mass was determined by weighing the graduated syringe before and after water filling and recording the difference. This quantity was readily converted to water volume representing the volume of the wax-coated soil. The volume of soil was obtained from the difference of volume of the wax coated sample and the volume of wax (mass/0.9). A 7.4% correction was applied to account for the underestimation due to air entrapment at soil–wax interface, as suggested by Prakash et al. (2008). The sample mass was also determined to estimate the bulk unit weight of the soil that, in turn, was converted to the void ratio using basic phase relationships.

3.4. Scanning electron microscopy

To correlate soil microstructure with engineering behavior, scanning electron microscopy (SEM) was performed using the microscope (JSM-6301FXV). The cryogenically prepared samples ensured an intact fabric and minimal grain re-adjustment (Lilly and Sargent, 1990). Each specimen (5 mm × 5 mm × 5 mm) was cut from the soil and immediately immersed in nitrogen slush at −208 °C for instantaneous freezing. The SEM chamber was flushed with argon to remove water vapor and vacuum cleaned with a rotary pump. Samples were placed in the chamber, sublimated at −40 °C, and examined at 2.5 kV till complete ice removal. An ablation depth of about 10 mm was obtained in approximately 45 min. Samples were gold sputtered in the cryogenic system at −155 °C to minimize ionization and transferred back to the chamber for visual examination. The vacuum pressure and scanning and recording speeds were 8×10^{-8} kPa, 450 frame/s and 40 s/frame, respectively. The 5 kV incident beam was kept at a vertical distance of 30 mm during photomicrograph capture. Soil morphology was observed through photomicrographs at representative locations.

4. Results and discussions

4.1. Geotechnical index properties

Table 1 summarizes the geotechnical index properties of the investigated soil. The field water content (w_f) and the dry unit weight (γ_d) were found to be 31% and 13.4 kN/m^3, respectively. From the measured specific gravity ($G_s = 2.75$) and degree of saturation ($S_f =$ 82%), the field void ratio (e_f) was calculated to be 1. The surface layer of the soil is highly affected by seasonal changes of water excess (snow melt in spring and precipitation in summer) and water deficiency (low rainfall and freezing in fall and winter). In the month of September when the samples were collected, indigenous soils generally experience a net water deficit given the semi-arid climate prevalent in the region. The high liquid limit ($w_l = 83\%$) and plastic limit ($w_p = 30\%$) along with a low shrinkage limit ($w_s = 15\%$) suggest the high water adsorbing and retaining capabilities of the clay. These values are attributed to the presence of expansive clay minerals in the soil. Fig. 1 that gives the grain size distribution (GSD) curve for the clay, indicates a clay size fraction (material finer than 0.002 mm) of 66%. Using the plasticity index ($I_p = 53\%$), the activity (A) of the soil was found to be 0.8, a value associated with moderate swelling. Based on the Unified Soil Classification System (USCS), the soil was classified as CH (clay with high plasticity).

Table 1
Summary of geotechnical index properties.

Property	Value
Field water content, w_f (%)	31.2
Field dry unit weight, γ_d (kN/m^3)	13.4
Specific gravity, G_s	2.75
Field void ratio, e_f[a]	1.05
Field degree of saturation, S_f (%)[b]	82
Liquid limit, w_l (%)	82.8
Plastic limit, w_p (%)	30.1
Plasticity index, I_p (%)	52.7
Shrinkage limit, w_s (%)	15
Clay size fraction, C (%)	66
Activity, $A = I_p/C$	0.8
USCS symbol	CH

[a] $e_f = (Gs\ \gamma_w/\gamma_d) - 1$.
[b] $S_f = w_f\ Gs/e_f$.

4.2. Water retention behavior

The SWCC that correlates water content with matric suction describes important features of soils when their saturation state is altered. Soils remain fully saturated with increasing suction up to the air entry value (AEV) when air starts to enter into pore spaces under the action of capillarity. Thereafter, soils continuously lose the capillary water with increasing suction until the residual state. The remaining adsorbed water is difficult to force out and complete soil desiccation requires 10^6 kPa suction. The curve composes of three straight-line parts: a horizontal line from saturation to the AEV; a steep downward slope from the AEV to the residual state; and a flat downward slope from the residual state to the completely dry state. The curve shape is affected by the following soil properties: (i) GSD and soil microstructure that influences pore connectivity and tortuosity; (ii) dry unit weight that is related to the total void space in a soil; and (iii) clay mineral types and amounts that dictate the amount of adsorbed water.

Fig. 2 gives the SWCC of the investigated clay with water content on the ordinate. Based on a unimodal equation (Fredlund et al., 2000), the estimated curve was obtained using geotechnical index properties (w, G_s, and γ_d) and the best fit of the measured GSD data (Fredlund et al., 2002). Based on a physico-empirical approach, the computer software of SoilVision Systems Ltd. divided the GSD into uniform particle sizes, each size assigned an individual SWCC

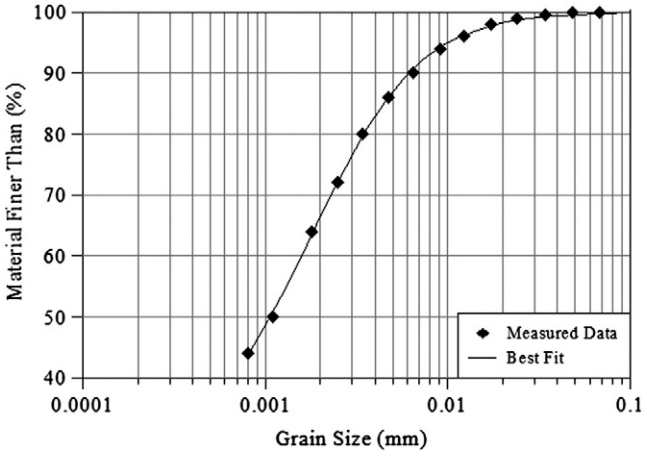

Fig. 1. Grain size distribution curve.

calculated from the database of measured SWCC, and all summed to develop the entire curve. The estimated SWCC followed the typical theoretical trend described above. The saturation water content equalling 38% remained constant up to the AEV of 300 kPa. Desaturation occurred at an increased rate between the AEV and the residual suction of 200,000 kPa (at w = 5%) and the curve finally joined the abscissa at 10^6 kPa under completely dry soil conditions.

The measured data fitted well to a bimodal distribution with two air entry values: a lower value (10 kPa) corresponding to drainage through fissures followed by a higher value (300 kPa) associated with seepage through the soil matrix. When the undisturbed samples were gradually desaturated, air first entered into the fissures at low suction. Although these fissures are partly sealed due to hydration of expansive soils (Azam and Wilson, 2006), numerous swell-shrink cycles over geologic time render these discontinuities to have much lower tensile strengths than the soil aggregates. This led to a quick drainage through these paths of least resistance. Subsequent application of suction affected the soil aggregates and eventually forced air to enter into the pore system of the aggregate. The matrix AEV matched the one obtained from GSD estimation because water movement through an aggregate is governed by the arrangement of individual particles. Furthermore, the downward SWCC shift of the undisturbed soil is attributed to its flocculated morphology in contrast to a dispersed fabric for the GSD sample (dispersion was ensured using sodium hexametaphosphate). The corresponding larger pores in the geologic samples were easy to dewater because of a reduced capillarity. This resulted in a greater water content reduction at the same matric suction. The data points between 10^4 kPa and 10^5 kPa suction measured by the chilled mirror potentiameter nicely captured the residual state and the two curves converged as the water present in both of the samples was electrochemically attached to the clay surfaces. The 5% residual water corresponded to the adsorbed water, as confirmed through thermogravimetric analysis (data not given in this paper).

Fig. 3 presents the soil water characteristics curve in the form of void ratio versus suction. The measured data closely approximated the estimated unimodal distribution based on GSD. The curve shows a single AEV of 300 kPa, become asymptotic to the abscissa after the residual value and never report to 10^6 kPa on complete drying. This is because void ratio of a soil pertains to an average value for all voids and does not differentiate between inter-aggregate fissures and intra-aggregate pores. Clearly, SWCC representation in the form of void ratio is not suitable for vertisolic expansive soils.

Fig. 4 gives the soil water characteristics curve in the form of degree of saturation versus suction. Similar to Fig. 2, the laboratory measured data depicted a bimodal function with a fissure AEV of 10 kPa and a matrix AEV of 6000 kPa. Due to reasons explained earlier, the matrix AEV matched the one obtained from GSD and the measured SWCC shifted downward. The average degree of saturation (S_{ave}) decreased due to drainage through fissures and reached 70% when most of the fissures were filled with air. Thereafter, the soil aggregates were difficult to drain and required a high suction (6000 kPa) for air to enter into the matrix. In contrast to Fig. 2, the significantly higher matrix AEV in this figure is attributed to the gradual decrease in soil volume with increasing suction. As explained later, this volume reduction is primarily due to reduced fissure sizes and, as such, was not captured in Fig. 3 that is based on an average void ratio.

The soil water characteristic curve given in the form of water content versus matric suction is the most accurate representation for vertisolic expansive soils. This is because the measured value of gravimetric water content captures the water drainage through fissures and is independent of volume changes due to water adsorption by clay particles. Likewise, the SWCC in the form of degree of saturation versus soil suction is most suitable for understanding volume decrease in fissures due to suction application. Marinho (2005) reported that for plastic soils, drainage through water filled pores is associated with pore compressibility due to capillarity and this phenomenon renders such soils to remain saturated over higher suction values. This representation implies that the expansive soil aggregates remain saturated over a wider range of suction generally prevalent in the field, as postulated by Fityus and Buzzi (2008).

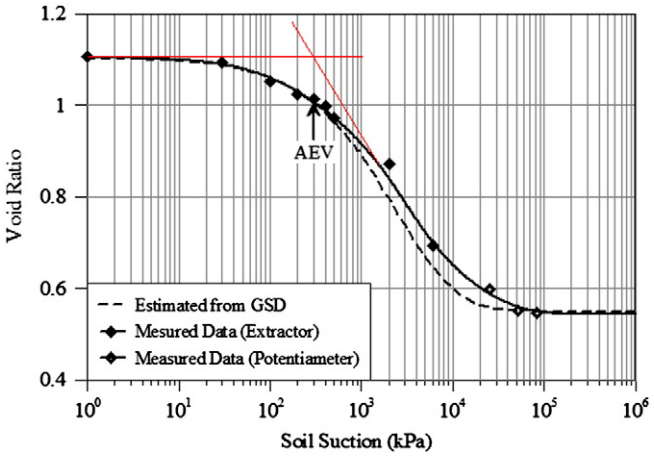

Fig. 3. Soil water characteristic curve in the form of void ratio versus soil suction.

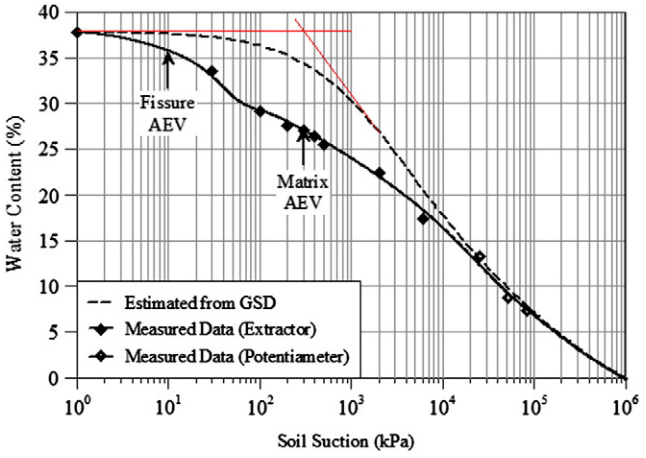

Fig. 2. Soil water characteristic curve in the form of water content versus soil suction.

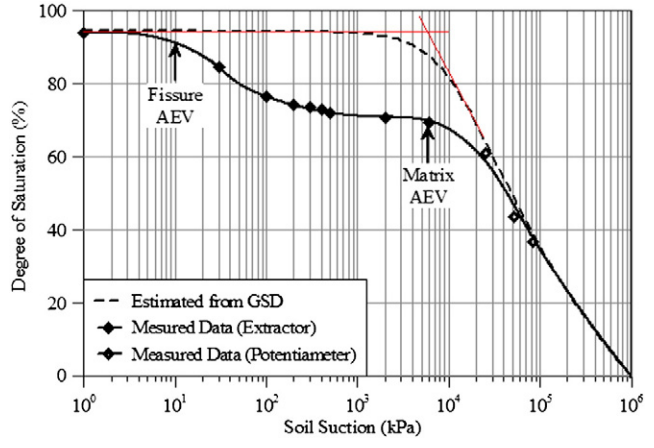

Fig. 4. Soil water characteristic curve in the form of degree of saturation versus soil suction.

4.3. Volume change behavior

Fig. 5 shows the swell-shrink path for the investigated clay. Theoretical lines representing various average saturation degrees were obtained from basic phase relationships and using $G_s = 2.75$. Field samples were first wetted to achieve complete saturation from an initially unsaturated state and subsequently desaturated by applying different suction values. The void ratio and water content of each sample were determined as described earlier in this paper.

The data depicted in Fig. 5 indicate an S-shaped curve representing the progressive drying (from e = 1.12 to e = 0.52) of the undisturbed soil. The curve composes of an initial low structural shrinkage followed by a sharp decline during normal shrinkage and then by a low decrease during residual shrinkage (Haines, 1923). During structural shrinkage, water within the fissures and some of the larger and relatively stable voids is removed such that the decrease in soil volume is less than the volume of water lost. Volume decrease in soil is equal to the volume of water lost during normal shrinkage thereby leading to a 45° straight line, which is almost parallel to the 100% saturation line. This suggests that drainage primarily takes place through the soil matrix in the normal shrinkage zone. During residual shrinkage, air enters the pores close to the shrinkage limit and pulls the particles together due to suction. This leads to a further decrease in soil volume albeit lower than the volume of water lost. Overall, the observed swell-shrink path is reversible because the soil has undergone numerous swell-shrink cycles since deposition. Tripathy et al. (2002) reported that equilibrium conditions are usually attained after about four cycles in compacted soils.

Theoretically, the swell-shrink path composes of two straight lines: a sloped line closely following the S = 100% line that joins a horizontal line at a void ratio associated with the shrinkage limit of the soil. This means that soils essentially remain saturated up to the shrinkage limit following a J-shaped curve. Due to the presence of fissures, the investigated soil exhibited deviations from this theoretical behavior. The field water content and the plastic limit were found to occur at $S_{ave} \approx 80\%$ up to which structural shrinkage (drainage through fissures) was found to dominate soil volume change albeit its absolute value was quite low. This also means that the matrix AEV (Fig. 2) does not occur at $S_{ave} = 100\%$ (as suggested by the SWCC estimated from the grain size distribution curve) but at a lower average saturation, as depicted by the laboratory measured data.

Studying the swell-shrink path for the investigated clay (Fig. 5) in conjunction with Table 1 indicated that the transitions between the various shrinkage stages correlate well with the consistency limits as follows: (i) structural shrinkage from the S = 100% line to the plastic limit; (ii) normal shrinkage from the plastic limit to the shrinkage limit; and (iii) residual shrinkage from the shrinkage limit to complete desiccation. The central linear portion of the swell-shrink curve representing only 20% change in saturation (from S = 80% to S = 60%) is associated with bulk of the volume changes in the investigated soil.

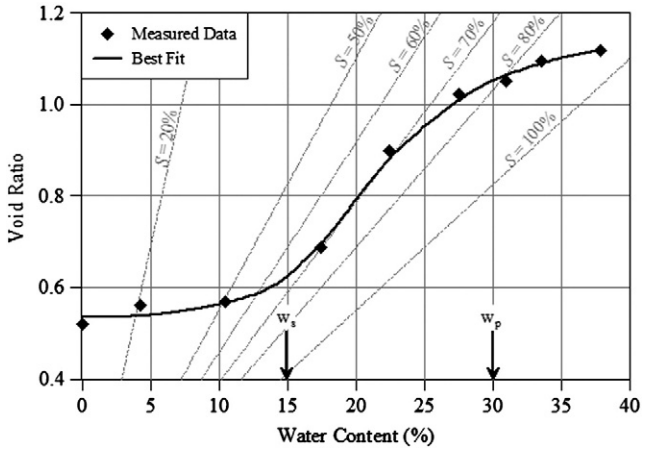

Fig. 5. Swell-shrink path.

The definition of the degree of saturation for vertisolic expansive soils is not straight forward. Since such soils consist of discontinuities and soil aggregates, the calculated degree of saturation pertains to an average value for the entire soil mass. This definition was used in Fig. 5 because it permits easy calculations. A more accurate approach is to consider only the soil aggregates as saturated up to the matrix AEV of Fig. 5 and the fissures as air filled cracks. This is close to an equilibrium field microstructure that allows alternate swelling and shrinkage (Ito and Azam, 2010). In this approach, the change of water volume in the soil mass equates to the volume change of the soil aggregates and that of the cracks. Gens and Alonso (1992) explained the two levels of soil structure in their framework as follows: the micro-level is governed by physicochemical interactions between the expansive clay minerals thereby forming aggregates whereas the macro-level includes both the aggregates and the fissures.

4.4. Soil microstructure

Fig. 6 illustrates the soil structure under saturated conditions. The specimen preserved the general features of vertisolic expansive soils, namely; fissuring and particle aggregations. The photomicrograph in Fig. 5a indicates the presence of permanent fissures of up to 10 μm width, which did not heal by water absorption even at full saturation. The random particle orientation is attributed to the geological deposition of the clay in a proglacial lake environment with high alkalinity and the presence of large amounts of multivalent ions (Ito and Azam, 2009). Fig. 6b indicates a flocculated fabric composing of flaky smectite clay particles oriented arbitrarily. This is related with clay swelling due to water adsorption such that the resulting deformations are experienced in all directions. The presence of multi-particle aggregates in the specimen is related to the stress dependent geologic history of the soil. Whereas the vertical swelling pressure is gradually canceled due to the overburden pressure, the lateral swelling pressure exerts shearing stress causing aggregate formation. The partly preferred orientation of clay particles along the skeletal grain (larger than clay particles and annotated as A) in this photomicrograph highlights the typical skelsepic plasma fabric of the soil.

Fig. 7 gives the soil fabric under in situ water content conditions (S = 82% and e = 1.05). This specimen appears to be quite similar to the previous one as depicted by the presence of clay aggregates and the comparable number and size of micropores. This is because an 18% decrease in saturation is associated with a change in void ratio of only 0.07 with very slight enlargement of hairline discontinuities shown in Fig. 7a. The in situ condition pertains to the matrix AEV (300 kPa) in Fig. 2 beyond which decrease in saturation is associated with large volume decrease given as normal shrinkage in Fig. 5. The emptied micro-scale discontinuities mean drainage through the fissures has occurred at a lower suction (10 kPa). This state also correlated well with the soil plastic limit (water content at which the soil begins to crumble) in which the entire soil mass containing the fissures is at a lower average saturation (80%) but the individual aggregates are completely saturated. Finally, the typical vosepic plasma fabric with preferred orientation alongside a planar void can be seen around an aggregate (denoted as A) in Fig. 7b.

Fig. 8 gives the soil morphology of the air-dried sample. This figure explains the observed desaturation and volume change behavior of the investigated vertisolic expansive soil when studied in conjunction with the previous specimens. Fig. 8a shows that although the fissures have widened up to 50 μm due to a low average degree of saturation of 21%, the clay fabric still appears to be quite packed (e = 0.56). This is attributed to the pulling together of clay particles due to suction during residual shrinkage that starts close to the shrinkage limit. When compared with Fig. 6b, the clay fabric clearly shows the

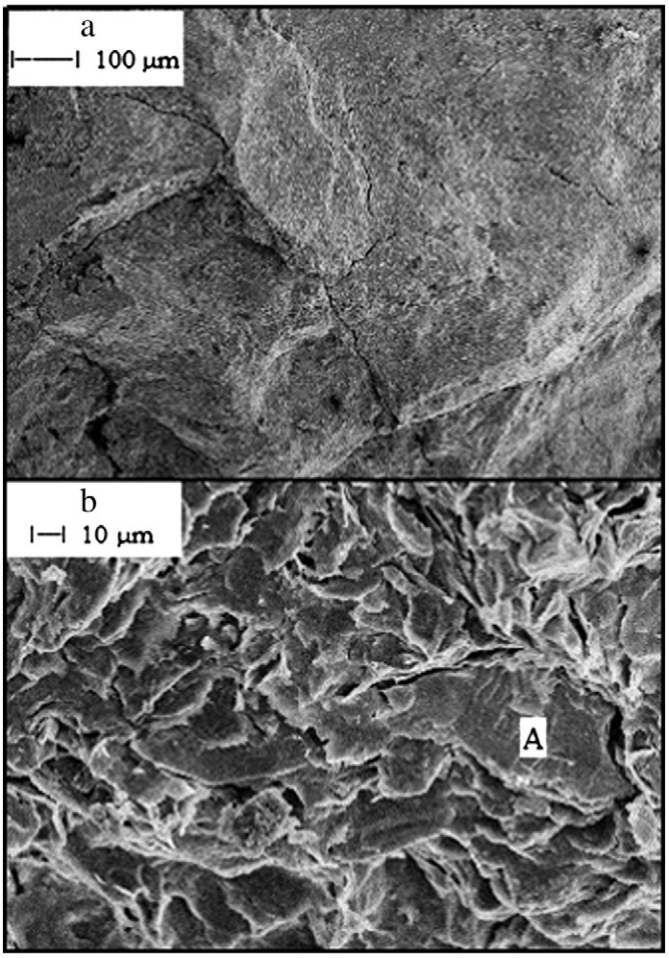

Fig. 6. Photomicrographs for saturated sample.

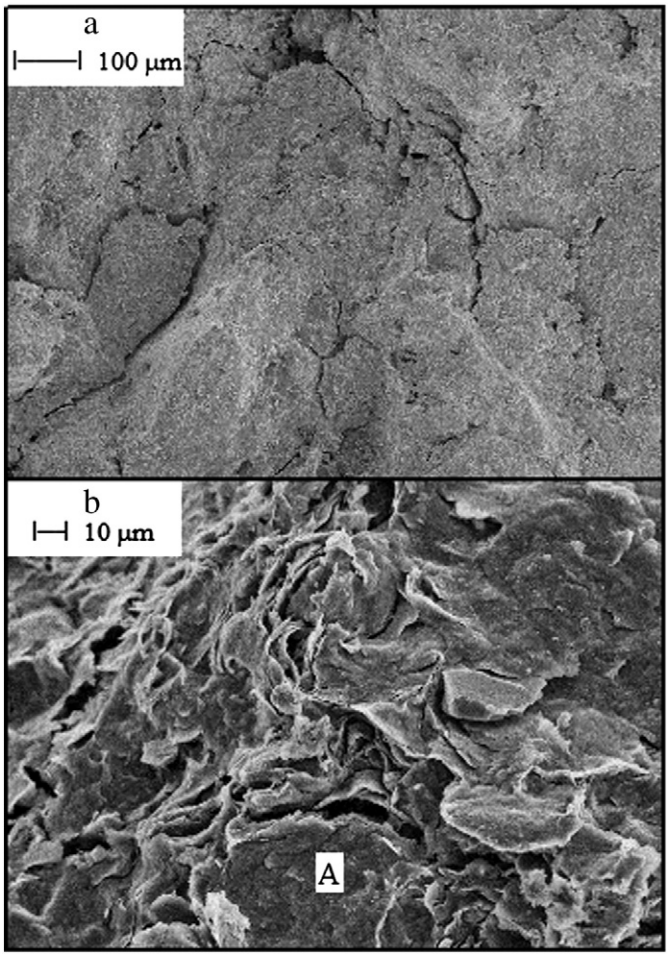

Fig. 7. Photomicrographs for in situ sample.

presence of numerous pore spaces and a considerable decrease in the aggregate size in Fig. 8b. The previously observed sepic plasma fabric due to clay swelling is now obscure by the rearrangement of clay particles during microstructural level desaturation. The decrease in aggregate size is attributed to the partial removal of adsorbed water from the clay.

The existence of fissures and multi-particle aggregates in all of the soil samples was confirmed for the investigated average saturation range of 100% through 20%. An equilibrium soil microstructure for the undisturbed samples mean that for the field conditions (up to the matrix AEV), the soil aggregates remain fully saturated whereas drainage primarily occurs through the fissures.

5. Summary and conclusions

Knowledge of the unsaturated soil properties is paramount for civil infrastructure construction in, on, or with expansive soils located in arid/semi-arid regions of the globe. Geologically induced fissuring and aggregation govern the engineering properties of the vertisolic expansive Regina clay. Laboratory investigations on undisturbed samples were conducted to develop a clear understanding of the geotechnical behavior of this local soil. The main conclusions of this research are summarized as follows:

- The investigated soil was characterized by a high clay content (66%) and classified as a clay with high plasticity. A high liquid limit (83%) and plastic limit (30%) along with a low shrinkage limit (15%) indicated a high water absorbing and retaining capacity of the clay.
- Water retention was characterized by a bi-modal SWCC distribution composing of a low fissure AEV (10 kPa) and a high matrix AEV (300 kPa based on water content and 6000 kPa based on the degree of saturation).
- The accurate way of representing SWCC for vertisolic expansive soils is to use the measured gravimetric water content whereas the SWCC representation using the degree of saturation is best suited to understand volume decrease in fissures due to suction.
- The swell-shrink path was found to be S-shaped and included a low structural shrinkage ($S = 100\%$ to $S = 80\%$ at w_p) followed by a sharp decline during normal shrinkage ($S = 80\%$ to $S = 60\%$ at w_s) and then by a low decrease during residual shrinkage ($S = 60\%$ to $S = 0\%$).
- Under in situ conditions (w_p and matrix AEV), the soil aggregates remain saturated while drainage occurs through the fissures. It follows that a change of water volume in the soil mass equates to the volume change of the soil aggregates and that of the cracks.
- The microstructure evolved over the investigated range of saturation (100% to 20%) and confirmed the typical features of vertisolic expansive soils, namely; fissures, multi-particle aggregates, random particle orientation, and sepic plasma.

Acknowledgments

The authors would like to gratefully acknowledge the financial support provided by the Natural Science and Engineering Research

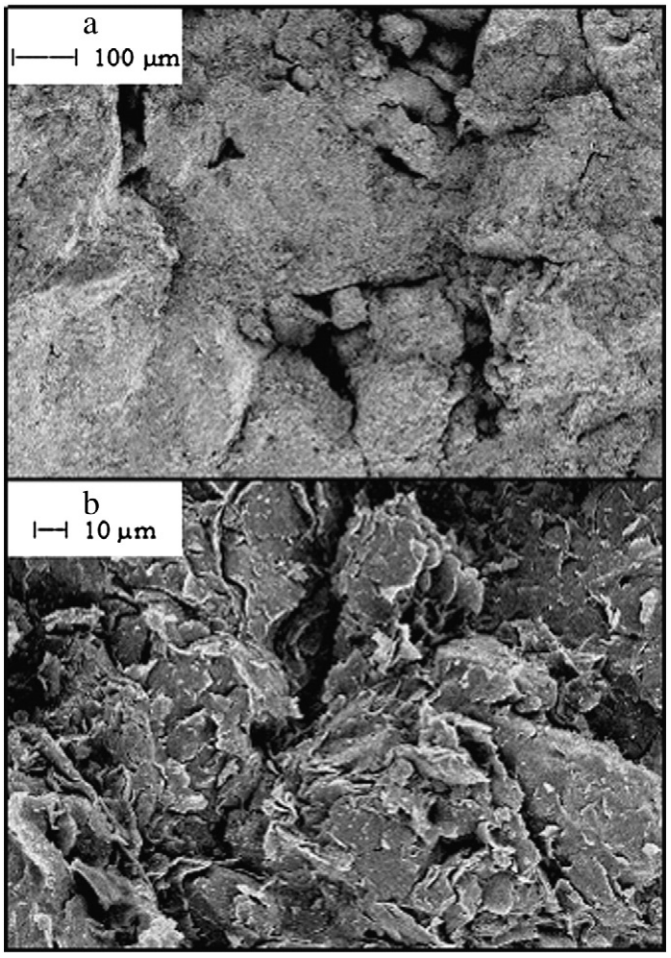

Fig. 8. Photomicrographs for air dried sample.

Council of Canada. Sincere thanks to the Saskatchewan Ministry of Highways and Infrastructure for providing material support, the University of Regina for providing laboratory space, and SoilVision Systems Ltd. for providing the computer software.

References

Ahmad, N., Mermut, A.R., 1996. Vertisols and Technologies for Their Management. Elsevier Science, New York, USA.

Azam, S., Ito, M., 2007. A Study on the Evaluation of Swelling Potential of Regina Clay Modified with Sand. Proceedings, 60th Canadian Geotechnical Conference, Ottawa, Canada, pp. 1907–1912.

Azam, S., Wilson, G.W., 2006. Volume change behavior of a fissured expansive clay containing anhydrous calcium sulfate. Proceedings, 4th International Conference on Unsaturated Soils, Carefree, Arizona, USA, 1, pp. 906–915.

Brackley, I.J.A., Sanders, P.J., 1992. In situ measurement of total natural horizontal stresses in an expansive clay. Geotechnique 42, 443–451.

Brierley, J.A., Stonehouse, H.B., Mermut, A.R., 2011. Vertisolic soils of Canada: genesis, distribution, and classification. Canadian Journal of Soil Science 91, 903–916.

Christiansen, E.A., Saure, E.K., 2002. Stratigraphy and structure of Pleistocene collapse in the Regina low, Saskatchewan, Canada. Canadian Journal of Earth Sciences 39, 1411–1423.

Cui, Y.J., Mantho, A.T., Martine, K.C., Audiguier, M., 2006. Water Retention Properties and Volume Change Behavior of Natural Romainville Clay. Proceedings, 4th International Conference on Unsaturated Soils, Carefree, Arizona, USA, 1, pp. 873–882.

Douglas, L.A., 1990. Micromorphology: A Basic and Applied Science. Development in Soil Science, 19. Elsevier, Amsterdam, The Netherlands.

Fityus, S., Buzzi, O., 2008. The place of expansive soils in the frameworks of unsaturated soil mechanics. Applied Clay Science 43, 150–155.

Fitzpatrick, E.A., 1993. Soil Microscopy and Micromorphology. John Wiley & Sons, New York, USA.

Fredlund, M.D., Fredlund, D.G., Wilson, G.W., 2000. An equation to represent grain-size distribution. Canadian Geotechnical Journal 37, 817–827.

Fredlund, M.D., Wilson, G.W., Fredlund, D.G., 2002. Use of the grain-size distribution for estimation of the soil–water characteristic curve. Canadian Geotechnical Journal 39, 1103–1117.

Gens, A., Alonso, E.E., 1992. A framework for the behaviour of unsaturated expansive clays. Canadian Geotechnical Journal 29, 1013–1032.

Haines, W.B., 1923. The volume change associated with variations of water content in soil. Journal of Agricultural Science 13, 296–310.

Hong, G.T. 2008. Earth Pressures and Deformation in Civil Infrastructure in Expansive Soils. Ph.D. Thesis, Texas A & M University, TX, USA.

Hu, Y., Hubble, D.W., 2005. Failure conditions of asbestos cement water mains. Canadian Geotechnical Journal 34, 608–621.

Ito, M., Azam, S., 2009. Engineering characteristics of a glacio-lacustrine clay deposit in a semi-arid climate. Bulletin of Engineering Geology and the Environment 68, 551–557.

Ito, M., Azam, S., 2010. Determination of swelling and shrinkage properties of undisturbed expansive soils. Geotechnical and Geological Engineering 28, 413–422.

Kelly, A.J., Sauer, E.K., Barbour, S.L., Christiansen, E.A., Widger, R.A., 1995. Deformation of the Deer Creek bridge by an active landslide in clay shale. Canadian Geotechnical Journal 32, 701–724.

Leong, E.C., Tripathy, S., Rahardjo, H., 2003. Total suction measurement of unsaturated soils with a device using the chilled-mirror dew-point technique. Geotechnique 53, 173–182.

Lilly, M.R., Sargent, J.A., 1990. Cryogenic Scanning Electron Microscopy Research Application in Arctic and Polar Regions. Proceedings, 9th International Conference of Offshore Mechanics and Arctic Engineering, Houston, Texas, USA, 4, pp. 51–60.

Marinho, F.M.A., 2005. Nature of soil–water characteristic curve for plastic soils. Journal of Geotechnical and Geoenvironmental Engineering 131, 654–661.

Mollard, J.D., Kozicki, P., Adelman, T., 1998. Some Geological, Groundwater, Geotechnical And Geoenvironmental Characteristics of the Regina Area, Saskatchewan, Canada. In: Karrow, P.F., White, O.L. (Eds.), Urban Geology of Canadian Cities. Department of Earth science and Quaternary Sciences Institute, University of Waterloo, ON, Canada.

Prakash, K., Shidharan, A., Baba, J.A., Thejas, H.K., 2008. Determination of shrinkage limit of fine-grained soils by wax method. Geotechnical Testing Journal 32, 86–89.

Tripathy, S., Subba Rao, K.S., Fredlund, D.G., 2002. Water content-void ratio swell-shrink paths of compacted expansive soils. Canadian Geotechnical Journal 39, 938–959.